ELSEVIER

Polymer Vol. 37 No. 8, pp. 1413–1430, 1996

0032-3861/96/$15.00+0.00

Morphology and crystal structure in single crystals of poly(*p*-phenylene terephthalamide) prepared by melt polymerization

J. Liu* and S. Z. D. Cheng
Institute of Polymer Science, University of Akron, Akron, OH 44325, USA

and P. H. Geil†
Department of Materials Science and Engineering, University of Illinois, Urbana, IL 61801, USA
(Received 26 June 1995)

Using the confined thin film melt polymerization technique lamellar single crystals, of two morphologies, have been grown for poly(*p*-phenylene terephthalamide). Electron diffraction (e.d.) patterns from these crystals and from fibre-like samples polymerized from sheared monomer, are in best agreement with a modified phase I cell. The lattice parameters ($a = 7.88$, $b = 5.22$, $c = 12.9$ Å; $\alpha, \beta, \gamma = 90°$) are similar to those in previously proposed cells, but the P1a1 space group rather than Pn or $P2_1/n$ space groups more closely fits the e.d. data. In particular, 210, 120, 320 and 410 reflections are present with moderate intensity, which are forbidden for the latter structures and do not result from double diffraction. Copyright © 1996 Elsevier Science Ltd.

(Keywords: electron diffraction; poly(*p*-phenylene terephthalamide); melt polymerization)

INTRODUCTION

The excellent mechanical properties and good thermal stability of poly(*p*-phenylene terephthalamide) (PPTA), as demonstrated by Kevlar[1], has generated considerable interest in the structure and morphology of this aromatic polyamide. Numerous techniques have been employed for obtaining an understanding of its crystal structure and properties including, e.g. wide-angle X-ray diffraction[2–6], electron microscopy and electron diffraction[6–11], small-angle X-ray diffraction using synchrotron radiation[12], atomic force microscopy[13], atomistic modelling[14,15], n.m.r. spectroscopy[16–19], i.r. spectroscopy[20,21], Raman spectroscopy[22], etc. These investigations, if not all, were made using PPTA fibres, films or as-polymerized bulk materials. To our knowledge there has been no report of single crystals of PPTA, although considerable effort has been devoted to attempting to grow them from solution[9,10]. Jackson and Chanzy[9] have described twisted ribbon-like crystals (molecular axis parallel to ribbon axis) for a high-molecular-weight PPTA and much smaller ribbons or platelets for a low-molecular-weight PPTA. In the latter the molecules were suggested to lie in the plane of the ribbon. The results of Takahashi *et al.*[10], for low-molecular-weight PPTA, were similar. Only fibre or powder electron diffraction (e.d.) patterns were obtained.

In this report, we describe the crystal structure and morphology of single crystals of PPTA prepared by a modification of our confined thin film melt polymerization (CTFMP) technique[23]. We have previously described its use for the preparation of a number of polyesters (e.g. poly(*p*-oxybenzoate)[23], poly(2,6-oxynaphthoate)[24], poly(4,4′-oxybibenzoate)[25], poly(*m*-oxybenzoate/2,6-oxynaphthoate)[26], poly(*p*-phenylene terephthalate)[27], and polybenzamide)[27], polyimides (poly(4,4′-oxydiphenylene pyromellitimide)[28], poly(1,4-phenylene-oxy-1,3-phenylene pyromellitimide)[29], poly-(1,4-phenylene-oxy-1,4-phenylene-oxy-1,4-phenylene pyromellitimide)[30]), a family of aromatic/aliphatic azomethine polyethers[31] and poly(terephthalate anhydride)[32]. Their lamellar (often ca. 100 Å thick) extended chain morphology permits the obtaining of *hk*0 single crystal e.d. patterns.

Based on X-ray techniques, two different monoclinic (pseudo-orthorhombic, $\gamma = 90°$) unit cells have been proposed for PPTA. Structures for phase (modification) I were proposed independently by Northolt (Pn)[2] and Tadokoro and coworkers ($P2_1/n$)[3,4] based on PPTA fibre X-ray diffraction. Phase II was prepared by dilute solution precipitation, with X-ray diffraction from films being used for the structure determination[5] (the e.d. patterns of Jackson and Chanzy are from modification I[9]). The reported crystallographic parameters of phases I and II are listed in *Table 1*. In the unit cells of the two modifications the proposed lattice parameters and chain conformations are nearly the same but the chain locations, and therefore the symmetry and

* Also at Department of Materials Science and Engineering, University of Illinois, Urbana, IL 61801, USA
† To whom correspondence should be addressed

Table 1 Crystallographic parameters of modifications I and II of PPTA

	Modification I[a,b]	Modification II[c]
a (Å)	7.87[a], 7.80[b]	8.0
b (Å)	5.18, 5.19	5.1
c (Å)	12.9	12.9
γ (deg)	90	90
Chain locations on a–b plane	[0,0]; [1/2, 1/2]	[0,0]; [1/2, 0]
Density (g cm^{-3})	1.48, 1.50	1.50
No. of chains in the cell	2	2

[a] Taken from ref. 2
[b] Taken from refs. 3 and 4
[c] Taken from ref. 5

space groups, are different (see *Table 2*). The crystal structures for phase I as proposed by Northolt[2] and Tadokoro and coworkers[3,4], based on a computer simulation, are shown in *Figure 6*.

Rutledge and Suter[14] have utilized atomistic modelling to simulate the molecular packing. Minimization of the intra- and intermolecular potential energy leads to eight different unit cells, with the polymorphism depending primarily on the nature of the packing between the hydrogen-bonded sheets. Four of the eight unit cells (nos 1–4) correspond to a phase-I-type packing, with nos 5–7 being related to phase II and no. 8 being a single-chain unit cell. They suggest that their models 3 and 4 are closest to their observations[15] of drawn, annealed (500°C, 2 s) PPTA fibres. However, both are close to hexagonal (i.e. $d_{110} \approx d_{200}$), with all spacings differing by 0.2 Å or more from that which these authors, ourselves, Northolt[2] and Tadokoro and coworkers[3,4] measure.

In this report, in addition to descriptions of the morphology of the CTFMP single crystals and their e.d. patterns, a different space group is proposed for phase I, based on our single crystal e.d. pattern. This lattice model has the same lattice constants and chain locations as the previous suggestions and a similar chain conformation, but a different lattice symmetry and space group. These differences are verified and demonstrated using computer modelling based on the Cerius[2] 1.6 program[33].

EXPERIMENTAL

Polymerization–crystallization of PPTA

The single crystals of PPTA were prepared by a modification of the CTFMP technique. A stoichiometric mixture of the two monomers, *p*-phenylene diamine (PPD) (Aldrich, $T_m = 144$°C) and terephthaloyl chloride (TCI) (Aldrich, $T_m = 80$°C) was made by mixing finely ground powders of a much larger amount of the two reactants than required for the CTFMP process. Instead of casting from solution as is normally performed[23–32], a small portion of the mixture was dispersed on a glass cover slip and then covered by another cover slip. In order to obtain fibre e.d. patterns, for determination of c, α and β, samples were also prepared by shearing the powder mixture on the cover slip at room temperature with a metal spatula before covering it. These sandwiched specimens were wrapped with aluminium foil and heated at 170°C for 3 h. The as-polymerized thin film of PPTA was rinsed with acetone to remove any residual monomer. Some specimens were subsequently annealed, on electron microscopy (EM) grids, in a differential scanning calorimetry (d.s.c.) cell under N_2 at higher temperatures. Solvent-cast films could not be used for the CTFMP technique, as the monomers reacted rapidly when their acetone solutions were mixed.

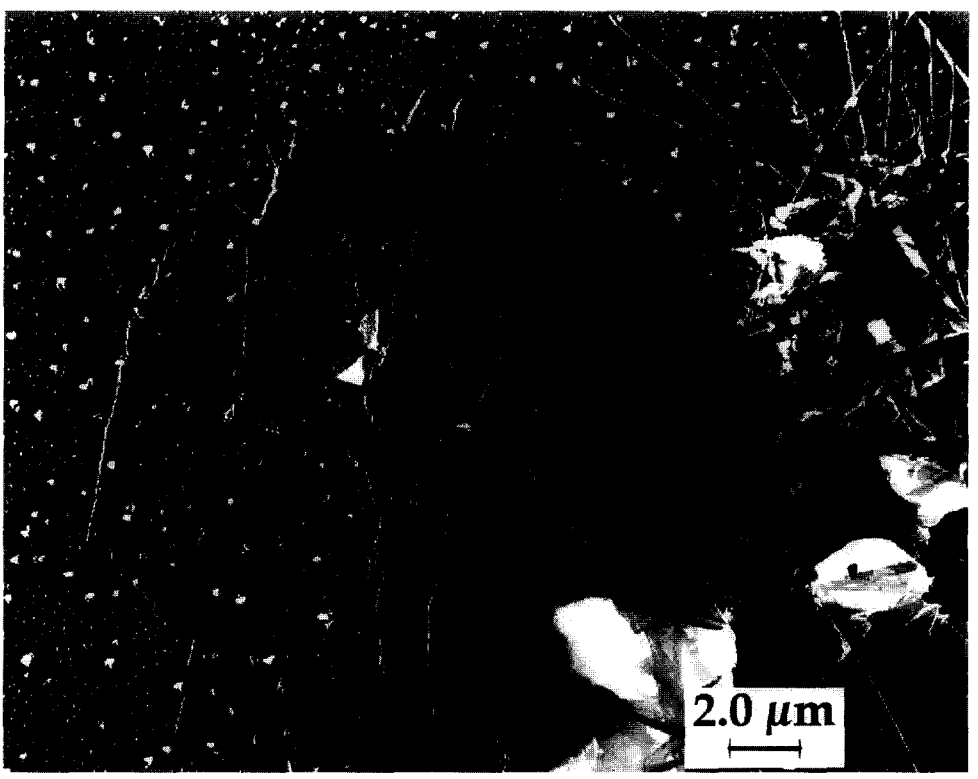

Figure 1 Planar crystal and lath crystals of PPTA polymerized at 170°C for 3 h; arrows indicate the regions where the planar crystal overlies the lath crystals

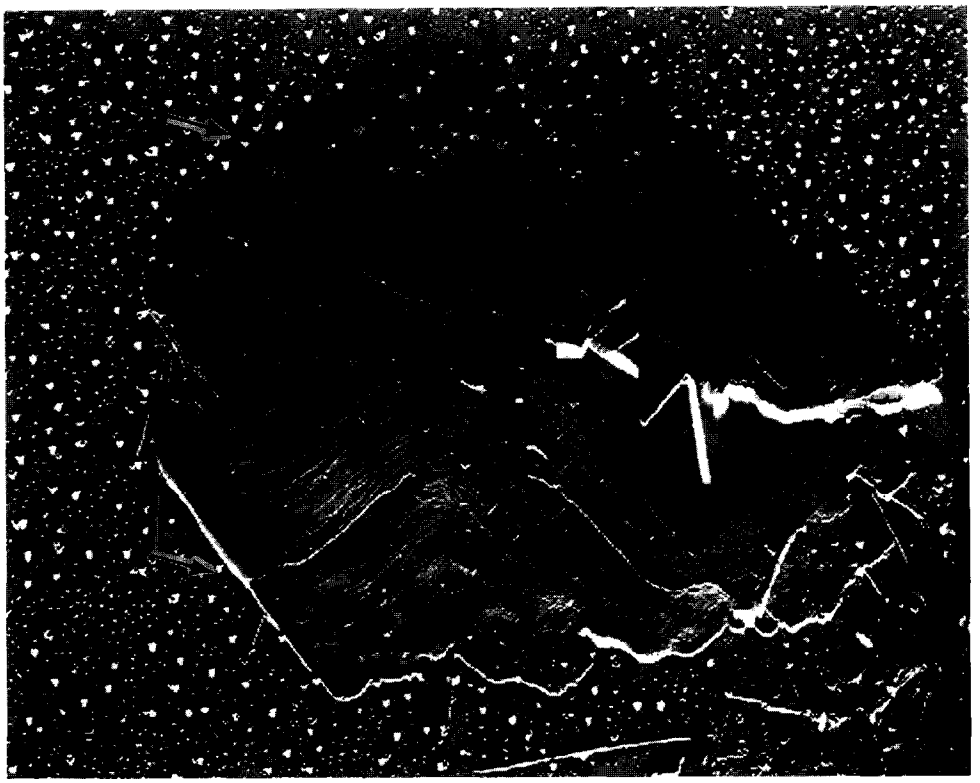

Figure 2 Twinned planar of crystal PPTAs polymerized at 170°C for 3 h; arrows indicate edges of the thickened central region which does not overlie the granular particles

Transmission electron microscopy and diffraction

The nascent PPTA samples were shadowed with Pt/C and coated with carbon in a vacuum evaporator. The micrographs and e.d. patterns were obtained on a JEOL-1200 II instrument operating at 120 kV or an Hitachi 600 machine operating at 100 kV. Low-dose techniques were commonly used for the observations. Spacings were measured using a Relysis scanner, in

Figure 3 Area of numerous lath crystals, after polymerization at 170°C for 3 h, followed by annealing at 400°C for 30 min

radial directions, including the Pt rings for calibration. Although the uncertainty using Pt is greater than if Au is used for calibration, the b/a ratio (1.31) is in excellent agreement with that reported by Northolt[2].

Computer simulation

The crystal structure of PPTA was simulated with the Cerius[2] 1.6 program from Molecular Simulations, Inc., using an IBM RISC 6000 workstation. The 2.11 version of the Dreiding force field was found to give 'better' results than the Universal force field also supplied with the program. In general, default options were chosen except in those cases where settings were recommended in the manual for polymer-type periodic systems.

RESULTS AND DISCUSSION

Single crystal morphology

Two different types of single crystals of PPTA were commonly observed, sword-like (smooth, tapered tip) lath-shaped crystals and planar crystals (*Figure 1*). As shown in *Figure 2* the planar crystals often have a twinned appearance and appear to be composed of numerous thin lamellae. The thickness of the lamella edges is ca. 15 Å, corresponding to one chemical repeat unit (TCI + PPD = 12.9 Å). Thinner layers, corresponding to one of the monomer units, might not be visible, hence we cannot discuss the relative reactivity of the groups. In both micrographs there is a thickened region in the centre of the crystal (edges denoted by arrows in *Figure 2*) with the outer regions of the crystal overlying several lath-shaped crystals (arrow in *Figure 1*) and a number of the granular particles distributed on the substrate. We thus suggest that the outer regions, at least, were formed out of contact with the substrate (i.e. in the molten film), being deposited on the substrate as the melt receded or residual monomer was removed with acetone.

Figure 3 shows a sample annealed at 400°C for 30 min, displaying a region containing many of the lath-shaped crystals. Annealing at 400°C did not appear to affect the morphology. Most of the laths have a thickness of ca. 100 Å, with a few of these appearing to be composed of two or more laths. As in the case of the planar crystals, the laths overlie each other, suggesting that they formed in the melt rather than on the substrate. As shown by e.d. (below), the molecular axes are normal to the lath surface; however, despite the high annealing temperature shear along the axes did not occur. The shadowing indicates that the overlying laths remain rigidly suspended for considerable distances.

Figure 4 shows a micrograph of a sample prepared from sheared monomer, where the general orientation is in the shear direction. A few short lath crystals are seen lying at random with, in addition, a number of short striations oriented normal to the shear direction. The origin and nature of these striations is not yet known. Furthermore, we have no confirmed explanation for the retention of the shear direction through the melting of the monomers; possibly, it is related to the 'rubbing' of the glass surface, which has been used to induce orientation of thermotropic liquid crystal polymers.

Electron diffraction

Figure 5a shows an [001] e.d. pattern from a planar crystal. The lath crystals yield similar patterns, with the long axis of the laths corresponding to the b-axis; this is the hydrogen-bonded direction. The strong 200 and 110 reflections suggest a Northolt–Tadokoro type crystal

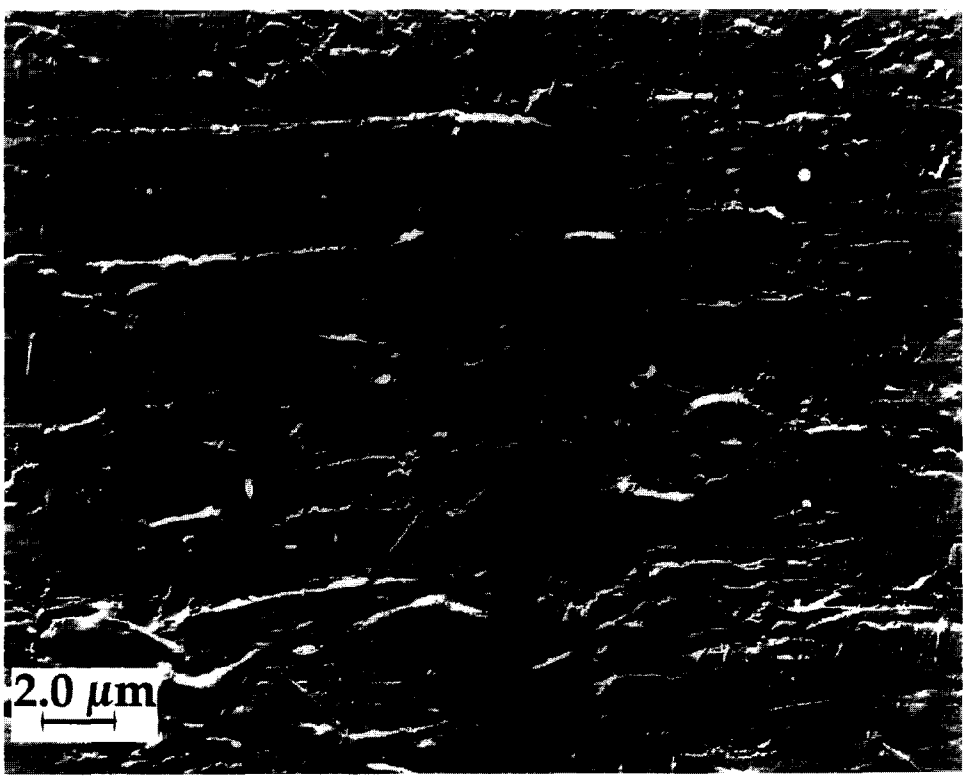

Figure 4 Sheared monomer polymerized at 170°C for 3 h and then annealed at 300°C for 30 min

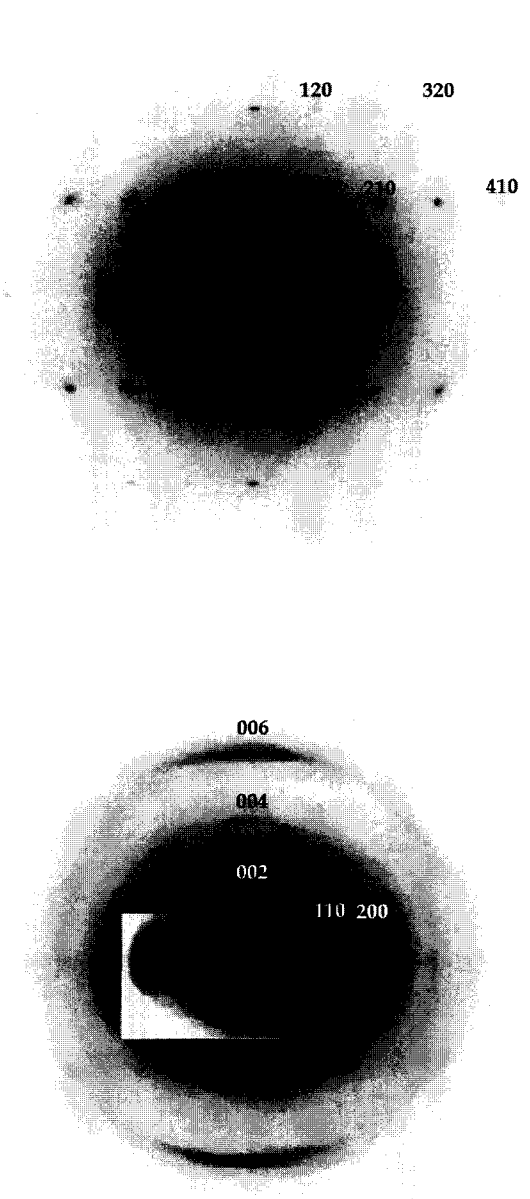

Figure 5 E.d. patterns from: (a) planar crystals as in *Figure 2*; (b) the sheared, polymerized, annealed monomer as in *Figure 4*

structure. The e.d. fibre pattern (*Figure 5b*), with 006 (strong), 002 (medium), and 004 (weak) meridional reflections is essentially the same as those reported previously[7–10]. Spacing and angle measurements indicate that these single crystals and fibres have the same lattice parameters as phase I (we have measured $a = 7.88$, $b = 5.22$, $c = 12.9$ Å; α, β, $\gamma = 90°$). The relative intensities of the reflections are listed in *Table 3*.

However, the relatively strong 210 reflections, as well as the weaker 120, 320 and 410 reflections, all of which are forbidden in both Northolt's Pn and Tadokoro and coworkers' $P2_1/n$ crystal structures, as well as, apparently, in Rutledge and Suters' models 3 and 4, and the medium 011 reflections, which were calculated by Northolt as being less than 0.1% of the 200 reflections, suggest that a re-examination of the crystal structure is appropriate. Northolt, in his paper, originally proposed a $P2_1/n$ space

Table 2 Space groups of PPTA modification I

Source	Northolt	Tadokoro group	This work
Brief name[a]	Pc	$P2_1/c$	Pc
Full name	P1 1n	P $112_1/n$	P1a1
Table no.	7	14	7
Lattice type	Monoclinic	Monoclinic	Monoclinic
Point group	m	2/m	m
Unique axis	*c*	*c*	*b*
	$\gamma = 90°$	$\gamma = 90°$	$\beta = 90°$

[a] Described as Pn, $P2_1/n$ and Pa, respectively, in the text

group, the full name presumably being $P112_1/n$, i.e. unique axis *c*, with this giving reasonable agreement with the observed intensities for a 500°C annealed fibre. This is the same space group symmetry proposed by Tadokoro and coworkers[3,4], although the conformation of the molecules, as shown in the diagrams, differ. However, Northolt indicated that he could obtain better agreement with the observed intensities, particularly for the 006, 004, 106, 104 and 105 reflections, all much stronger than calculated, by a slight (0.32 Å) shift along the *c*-axis between the hydrogen-bonded planes of the molecules, resulting in the reduction in symmetry to Pn. The Cerius[2] simulated unit cell, with this shift and using his parameters, and the corresponding e.d. fibre and *hk*0 ([001]) single crystal patterns are shown in *Figures 6* and *7*. (Northolt's cell was simulated with space group $P112_1$ and then shifting the centre chain by 0.32 Å. It is noted that the $P112_1$ space group symmetry was used to build the unit cell, with the $P112_1/n$ symmetry yielding four molecules per cell, two of each superimposed at the centre and corners). *Table 3* lists the observed and calculated X-ray intensities, as tabulated by Northolt, and the X-ray and e.d. intensities based on our simulated unit cell, as calculated by the Cerius[2] program.

The variation in calculated intensities is due, in part, to the different C/O scattering factor ratios for X-ray and electron radiation ($O/C_{X\text{-ray}} = 1.62$, $O/C_{e.d.} = 1.06$ at $\sin(\theta/\lambda) = 0.25$, i.e. $d = 2$ Å). Northolt used a temperature factor of 5 Å^2; the same factor was used for all of the X-ray and e.d. intensities calculated by the Cerius[2] program. A Lorentz-polarization factor is included for the X-ray calculations but not for the e.d. ones.

Northolt also examined a PPTA fibre annealed at 400°C. For this sample he indicates that weak *hk*0 reflections with $h + k$ odd were observed (forbidden in the Pn and $P2_1/n$ space groups), as well as a 'change in the relative intensity for most of the reflections'. Other than for the photo, data for these samples was not given. He did conclude, however, despite getting better agreement for the 500°C annealed sample with the staggered Pn symmetry, that 'the most favourable symmetry may indeed be $P2_1/n$'.

Prior to publication of Northolt's paper, Hasagawa *et al.*[3] also proposed a $P2_1/n$ space group. Although not published, the results were summarized in a subsequent paper from Tadokoro's group[4]. This is essentially the same $P2_1/n$ monoclinic unit cell, (unique axis *c*, $\gamma = 90°$) assumed by Northolt. In the crystal structure described by Tadokoro and coworkers the molecules have a twofold screw symmetry and all-*trans* internal rotation angles. Because of the symmetry of the molecule, the centre chain is related to the corner

Table 3 Observed and calculated intensities for the proposed PPTA space groups[a]

		Pn			$P2_1/n$		Models 3 and 4 (ref. 15)			Pa		
hkl	I_O[b]	I_c (X-ray)[c] (%)	I_c (X-ray)[d] (%)	I_c (e.d.)[e] (%)	I_c (X-ray)[d] (%)	I_c (e.d.)[e] (%)	I_O[b,f] (%)	I_C (3, X-ray) (%)	I_C (4, X-ray) (%)	I_o	I_C (X-ray)[g] (%)	I_c (e.d.)[g] (%)
200	vs (100)	100 (100)	100	100	100	100	100	100	100	vs	100	100
400	w (1)	1 (1)	1.8	3.0	1.8	3.0		–	–	w	0.8	2.1
01$\bar{1}$	vw	<<	0.1	0.03	0.07	0.01		0	2	m	4.8	2.1
01$\bar{1}$				0.03		0.01		0	4	w		2.1
020	vw	<	0.5	1.3	0.5	1.3		0	0	w	0.6	1.1
022	m (4)	1	2.1	4.1	2.2	4.3		–	–	w	1.8	3.7
002	m (7)	9 (9)	0.3	3.3	0.4	3.5	3	5	5 (78°)	m	0.4	3.9
003	n.o.		0.02	0.01	0	0					0.3	0.2
004	s (30)	32 (32)	4.7	0.9	5.7	1.0	12	13	17 (78°)	w	6.7	1.2
005	vw	1 (1)	0.2	0.1	0	0		0	0	n.o.	0.7	0.4
006	s	22 (22)	12.3	7.0	18.9	10.8	26	9	17 (78°)	s	22.2	12.2
110	vs (81)	72 (36)	60.2	31.9	60.2	31.9	81 (40)	74	50	s	80.0	42.6
$1\bar{1}0$				38.3		38.3		23	21	s		42.6
210	n.o.	0	0	0	0		0	0		w	8.1	3.8
310	m (4)	4 (2)	8.1	6.5	8.1	6.5	10 (5)	37.7	37.3	m	10.5	10.0
$3\bar{1}0$				12.3		12.3		36.7	37.7	m		10.0
410	n.o.	0	0	0	0		0	0		vw	0.1	0
510	vw	<	0.5	0.3	0.3	0.5	0.3	–	–	n.o.	0.9	1.3
$5\bar{1}0$				1.4		1.4		–	–	n.o.		1.3
120		0	0	0	0	0		0	0	vw	0.1	0.3
220	w	<	0.2	0.2	0.2	0.2		–	–	n.o.	0.2	0.2
$2\bar{2}0$				0.04		0.04		–	–	n.o.		0.2
320	n.o.		0	0	0	0		0	0	vw	0.1	0.5
420	w–m (1)	1 (0.5)	1.2	2.6	1.2	2.6		-	-	w	1.0	1.4
$4\bar{2}0$				1.4		1.4		-	–	n.o.		1.4
620	w	<	0.4	1.0	0.4	1.0		–		n.o.	0.3	0.4
130	n.o.	<<	0.01	0.1	0.01	0.1		-		n.o.	0.02	0
$1\bar{3}0$				0.01		0.01		–	–	n.o.		0
330	vw	<	0.2	0.01		0.01		–	–	n.o.	0.1	0.1
$3\bar{3}0$				0.3		0.3		–	–	n.o.		0.1
101	n.o.	<<	0.04	0.03	0.04	0.03		0	3 ($\bar{1}$01)	n.o.	0	0
102	n.o.	<	0.01	0.05	0	0		–	-	n.o	0	0
103	n.o.	<	0.3	0.2	0.2	0.1		0	2 (103)	n.o.	0	0
									1 ($\bar{1}$03)			

104	w	2	0.8	0.2	0.02	0		–	–	n.o.	0	0
105	n.o.	<	0.5	0.3	0.4	0.2		–	–	n.o.	0	0
106	s (11)	7	5.4	3.0	0.2	0.1	15 (8)	4	0	n.o	0	0
111	s (8)	8 (4)	5.3	1.4	5.2	1.3		1	0	n.o.	0.9	0.8
$1\bar{1}1$				1.8		1.7		2	0	n.o.		0.8
112	w	1	0.8	0.4	0.7	0.4		0	2	n.o.	0.2	0.1
113	w–m	3	2.6	1.1	2.7	1.2		0	0	n.o.	1.1	0.4
114	w	2	2.9	1.6	2.9	1.7		0	3 ($1\bar{1}4$)	n.o.	2.1	0.7
201	n.o.	<<	1.0	0.5	1.0	0.5		2	0	n.o.	6.7	10.2
202	w	3	2.2	0.5	2.3	0.5		0	2	n.o.	1.0	0.3
203	n.o.	<	1.1	0.8	1.2	0.9		2	0	n.o.	3.8	0.6
211	s (14)	17 (8)	19.6	16.8	19.8	16.9	23 (12)	4	14	m	20.8	21.2
211				15·0		15·2		5	13	m		21·2
212	n.o.	1	1.3	0.4	1.3	0.4		–	–	n.o.	2.6	0.1
213	w	2	1.9	0.8	1.9	0.8		0	2	n.o.	1.3	0.4
214	n.o.	1	1.6	1.2	1.6	1.1		–	–	n.o.	3.2	0.02

[a] I_O, observed intensity; I_c, calculated intensity; n.o., not observed; –, not listed; <, $0.1 < I_{calc} < 0.5$;<<, $I_{calc} < 0.1$
[b] Values in ( ) are integrated intensities taken from azimuthal and radial diffractometer scans
[c] As calculated by Northolt[2]; ( ) are values corrected for multiplicity
[d] Calculated X-ray fibre pattern intensity by Cerius[2]
[e] Calculated single crystal electron diffraction intensity by Cerius[2], these values correspond to F^2, corrected for the temperature factor
[f] Additional reflections observed (2θ, β, I): 29.8°, 74°, 5; 33.4°, 57°, 5; 49.9°, 0°, 8
[g] As modified from minimized packing, see text for details

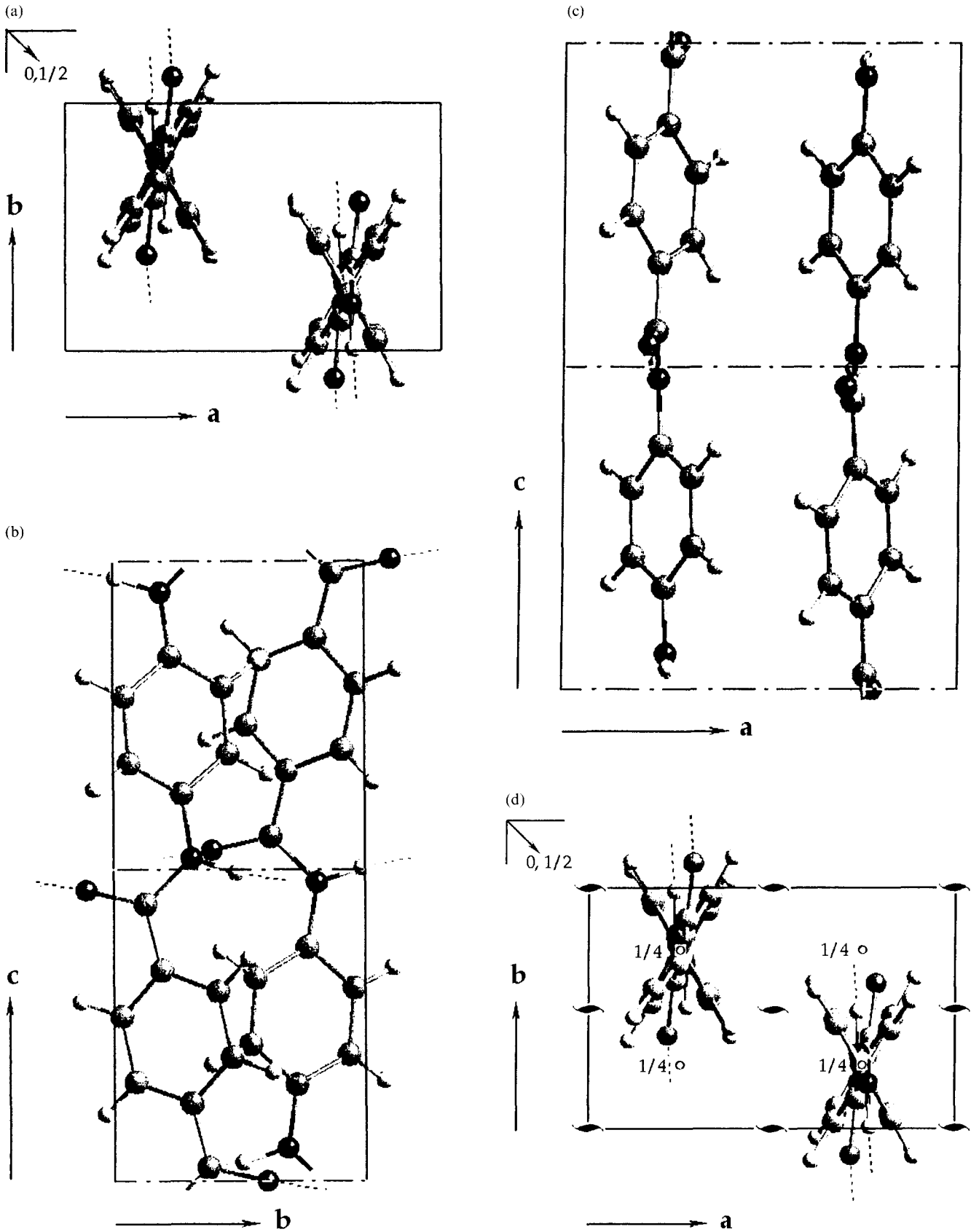

Figure 6 Simulated crystal structure for PPTA based on Northolt's Pn[2] and Tadokoro and coworkers' $P2_1/n$[3,4] unit cells: (a) [001] projection for Pn cell; (b) [100] projection for Pn cell; (c) [010] projection for Pn cell; (d) [001] projection for $P2_1/n$ cell; (e) [100] projection for $P2_1/n$ cell; (f) [010] projection for $P2_1/n$ cell

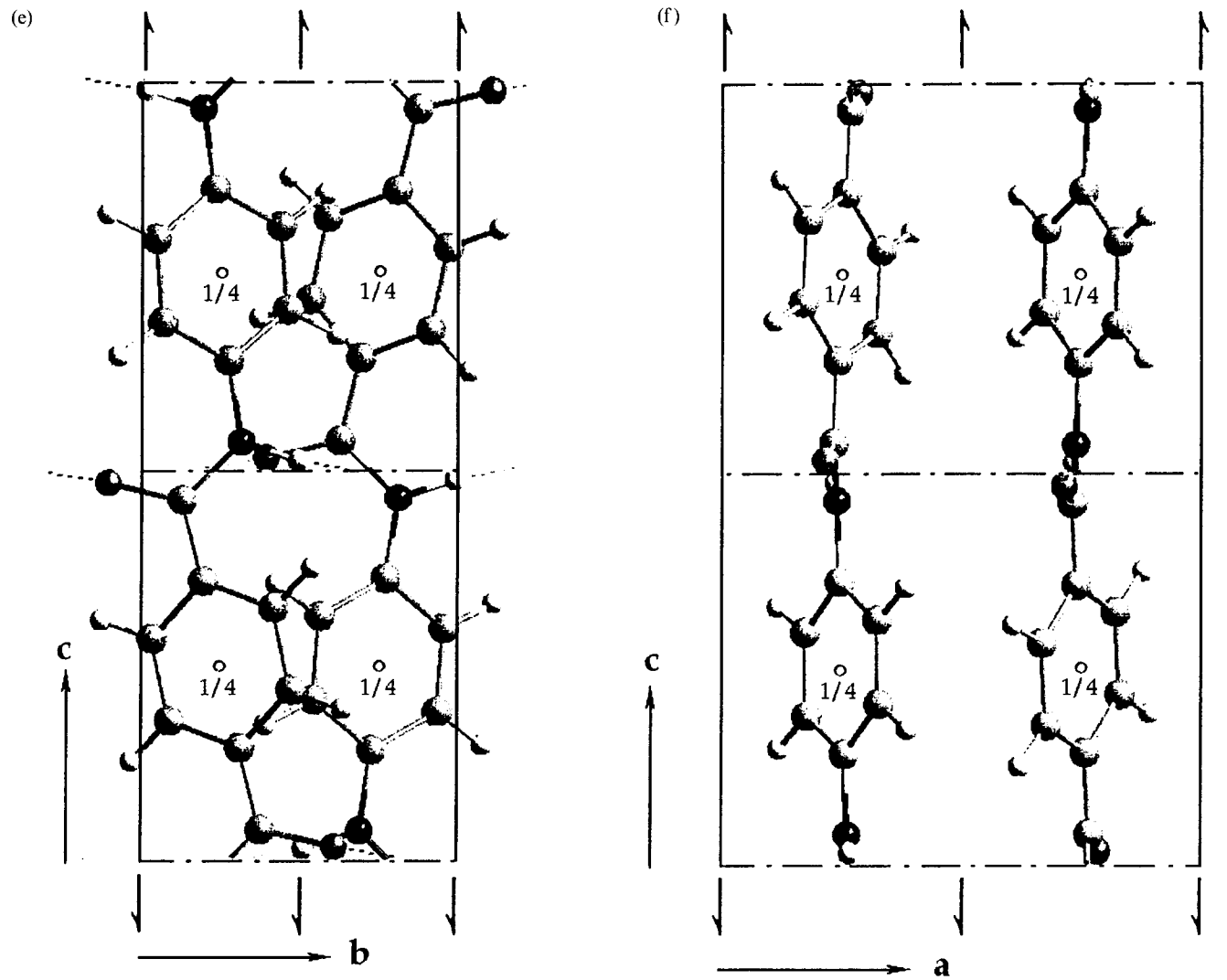

Figure 6 (*Continued*)

chain by a translation of $1/2\,c$ along the c-axis or by an n-glide plane at $z = 1/2\,c$ with a glide of $1/2\,(a + b)$. The simulated unit cell is shown in *Figures 6d–f* with the symmetry elements displayed. It is identical to that shown in *Figures 6a–c* except for the stagger (in *Figure 6b* the left-hand molecule has been shifted down, and the right-hand molecule up by about 2/3 the diameter of the hydrogen atom on the n-glide plane at $1/2\,c$).

The e.d. intensities calculated by Cerius[2] for 'Tadokoro's cell'[3,4] are also listed in *Table 3*, with the simulated e.d. fibre pattern shown in *Figure 7c*. In both Northolt's and Tadokoro and coworkers' cell the [001] projections are identical. The amide and carboxyl groups in the two molecules are aligned parallel to each other, at an angle of about 4° to the b-axis. The $h + k$ odd reflections, as indicated in the table, are completely absent in the simulated $hk0$ pattern.

In both of the above cells calculated values for pairs of reflections such as $hk0$ and $h\bar{k}0$, are different; this results from the parallel orientation of the NH–CO planes. While this effect would not be observed in X-ray patterns (fibre or powder) the asymmetry should be observable by e.d. from single crystals unless there is multiple, small-scale twinning. We have not observed this effect for PPTA, although a related asymmetry has been observed for liquid crystal polymers containing two bromine groups[35].

Also listed in *Table 3* are the observed (annealed fibre) and calculated (for models 3 and 4) X-ray intensities as listed by Rutledge *et al.*[15]. As noted above, the unit-cell parameters ($a = 8.3$, $b = 5.0$, $c = 13.1$ Å, $\alpha = \beta = 90°$, $\gamma = 92°$ for model 3; $a = 8.4$, $b = 4.9$, $c = 13.1$ Å, $\alpha = 86°$, $\beta = 78°$, $\gamma = 89°$ for model 4) differ from those observed, with model 3 being the closest. A 5 Å^2 temperature factor was also used in their calculations.

The clear 210, 120, 320 and 410 reflections in our $hk0$ e.d. patterns led us to consider an alternate symmetry, namely an a-glide plane. The a-glide symmetry operation introduces two chains with the same conformation in the [100] projection (see *Figure 8b*), but without the $1/2\,c$ translation resulting from the 2_1 screw operation; all of the centrosymmetries of the 2_1 screw, however, are maintained. The simulation, using the Dreiding 2.11 force field, but modified as below, is shown in *Figure 8*, using the same lattice parameters as for *Figure 6*. This a-glide symmetry corresponds to a P1a1 (brief name Pa) space group. It is a monoclinic lattice with unique axis b, and $\beta = 90°$.

The corresponding simulated e.d. patterns and an X-ray fibre pattern are shown in *Figure 9*. In [001] projection a

(a)

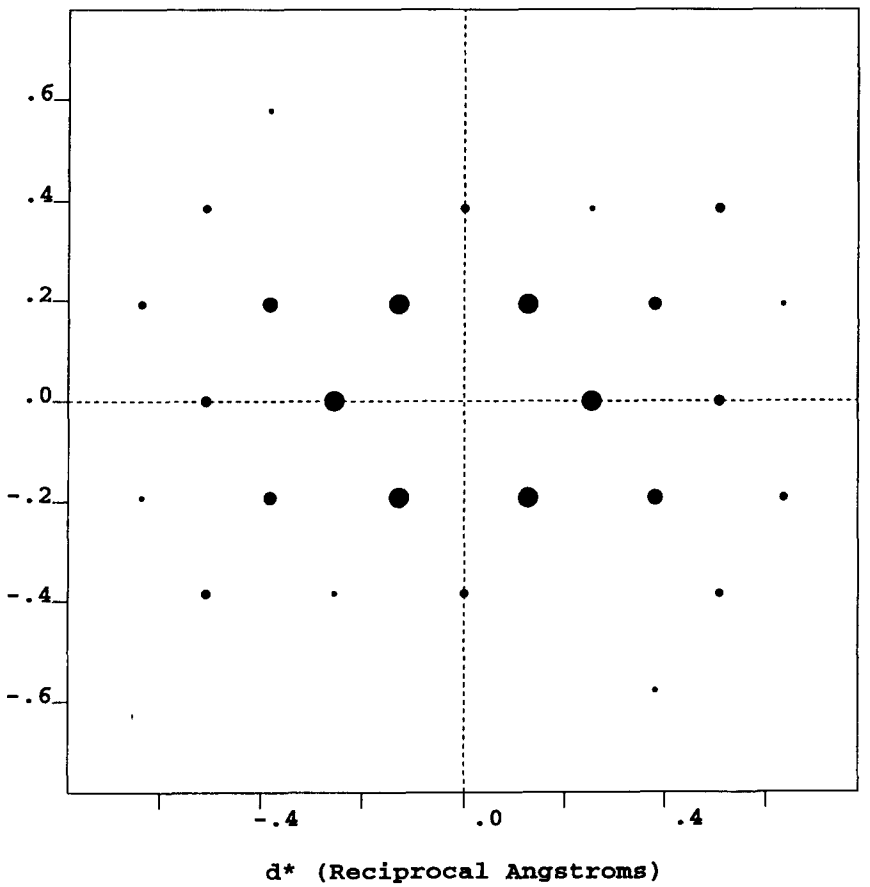

(b)

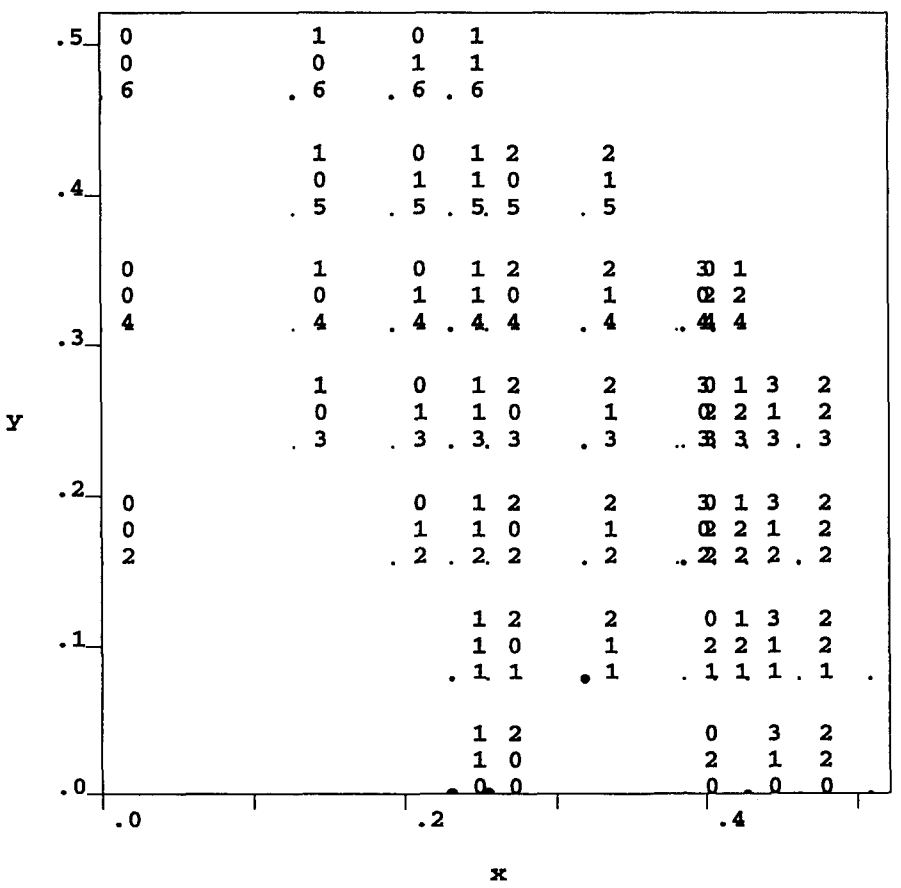

Figure 7 Simulated PPTA e.d. diffraction patterns based on the unit cells in *Figure 6*, assuming a 500 Å lateral crystal size, 50 Å thickness (*c*-axis) for the *hk*0 pattern and 500 Å thickness for the fibre patterns: (a) simulated *hk*0 e.d. pattern based on *Figures 6a* and *d*; (b) simulated e.d. fibre pattern based on *Figures 6a–c*; (c) simulated e.d. fibre pattern based on *Figures 6d–f*

(c)

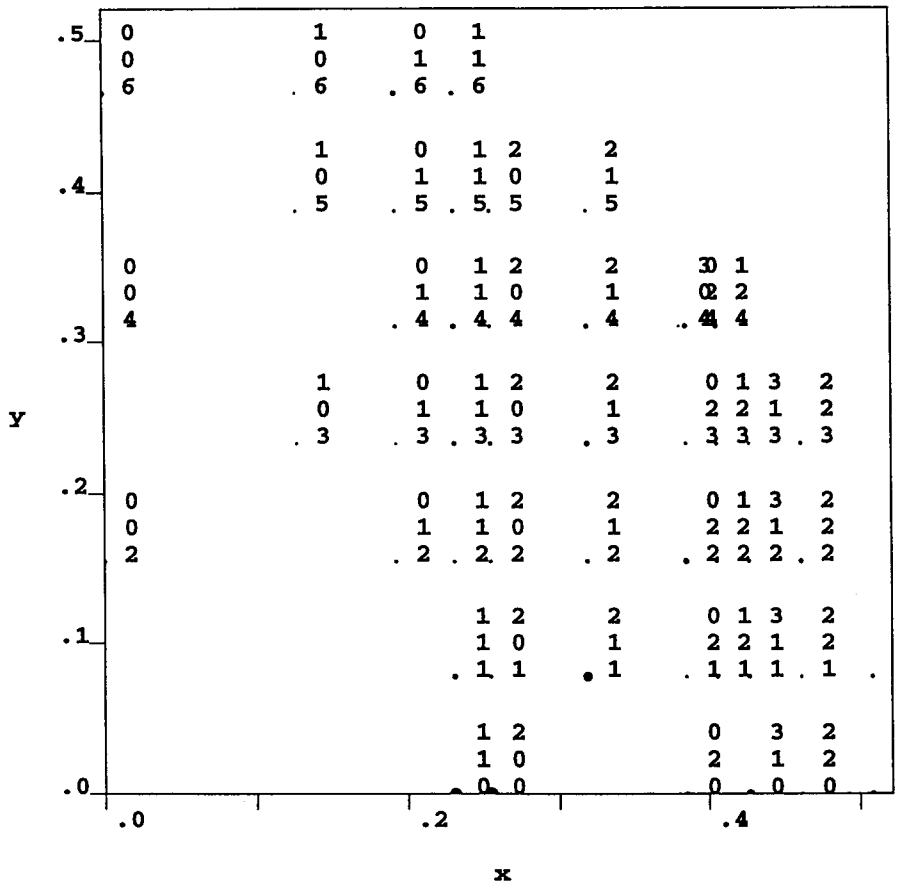

Figure 7 (*Continued*)

geometrically symmetric structure, including the hydrogen bonds (*Figure 8a*), is produced, resulting in a symmetric [001] e.d. pattern (*Figure 9a*). The $(h + k)$ odd reflections, in particular 210, 120, 320 and 410, are present with their relative intensities in good agreement with that observed. In addition 003 (weak), 005 and 011 are proposed, while $10l$ are absent (*Figure 9b*). With this space group symmetry the corresponding atoms in the two chains have the same z-coordinates along the c-axis; the $1/2\,c$ differences in the Northolt–Tadokoro models do not occur.

The model shown in *Figure 8* does not correspond to the minimum energy structure based on the Dreiding force-field; the 210, etc. reflections for the minimum energy model were too weak. The setting angle for the phenyl rings in the minimized model was about the same as in *Figures 6a* and *d*. Rigidly rotating the molecules about the c-axis, the left-one clockwise, the right-one equally counter-clockwise by $\sim 12°$, results in better agreement with the observed e.d. pattern. After the rotation the O–H bond length increased slightly to 2.328 Å with the N–H–O bond angle being 155.2°. The corresponding values for our simulation of the Northolt–Tadokoro cells are 2.124 Å and 172°. Our values are close to the average values obtained by Rutledge and Suter in their modelling (2.3 Å, 160°), values which they claim are appropriate for PPTA[14]. E.d. and X-ray intensities for the modified cell are listed in *Table 3*. They agree well with our observed values.

It is noted that there are four space groups, Pa, Pb, $P12_11$, and Pn11, that can generate the same [001] projection in molecular packing , and thus give the same [001] e.d. pattern, i.e. with $h + k =$ odd reflections (210, 120, 320, 410, etc.). $P2_111$ and P1n1 also could give the same [001] projection, but minimization using the Cerius Crystal Packer results in transformation to a phase-II type packing. The four cells listed all minimize to phase I. Therefore, the final choice of space group for PPTA phase I has to be based on the observation of a fibre pattern. Based on our Cerius[2] simulation, all of the space groups except Pa introduce the $10l$ reflections in both X-ray and electron diffraction patterns, although the individual intensity varies. The lack of $10l$ reflections is in agreement with our e.d. fibre pattern, which, however, is relatively weak, with considerable breadth to the arcs. This also agrees, it is believed, with the e.d. fibre patterns in refs 9 and 10, but differs from the e.d. patterns of Dobb *et al.*[7], who claim a strong 106 (from sections of pleated sheet fibres). In addition, Northolt[2] and Rutledge *et al.*[15] list 106 for their X-ray patterns (*Table 3*). Although 106 and the other $10l$ reflections are extremely weak in the Pa space group, as in the case of Northolt's results, shifting of the hydrogen-bonded planes results in an increase in their intensity. Furthermore, the Pa and Pb models give 211 reflections with medium intensity ($\sim 30\%$ of the 200 intensity) which is observed in our e.d. fibre pattern and in refs 9, 10 and 15, but the other two models show much weaker ones ($\sim 1\%$ or less of the 200 intensity); this excludes the $P12_11$, and Pn11 models. Finally, the observed weak 011 reflection in the e.d. fibre pattern (also ref. 15), forbidden for the Pb model, would also suggest Pa is correct. The simulated quadrant e.d. fibre patterns of the four space groups with the same chain

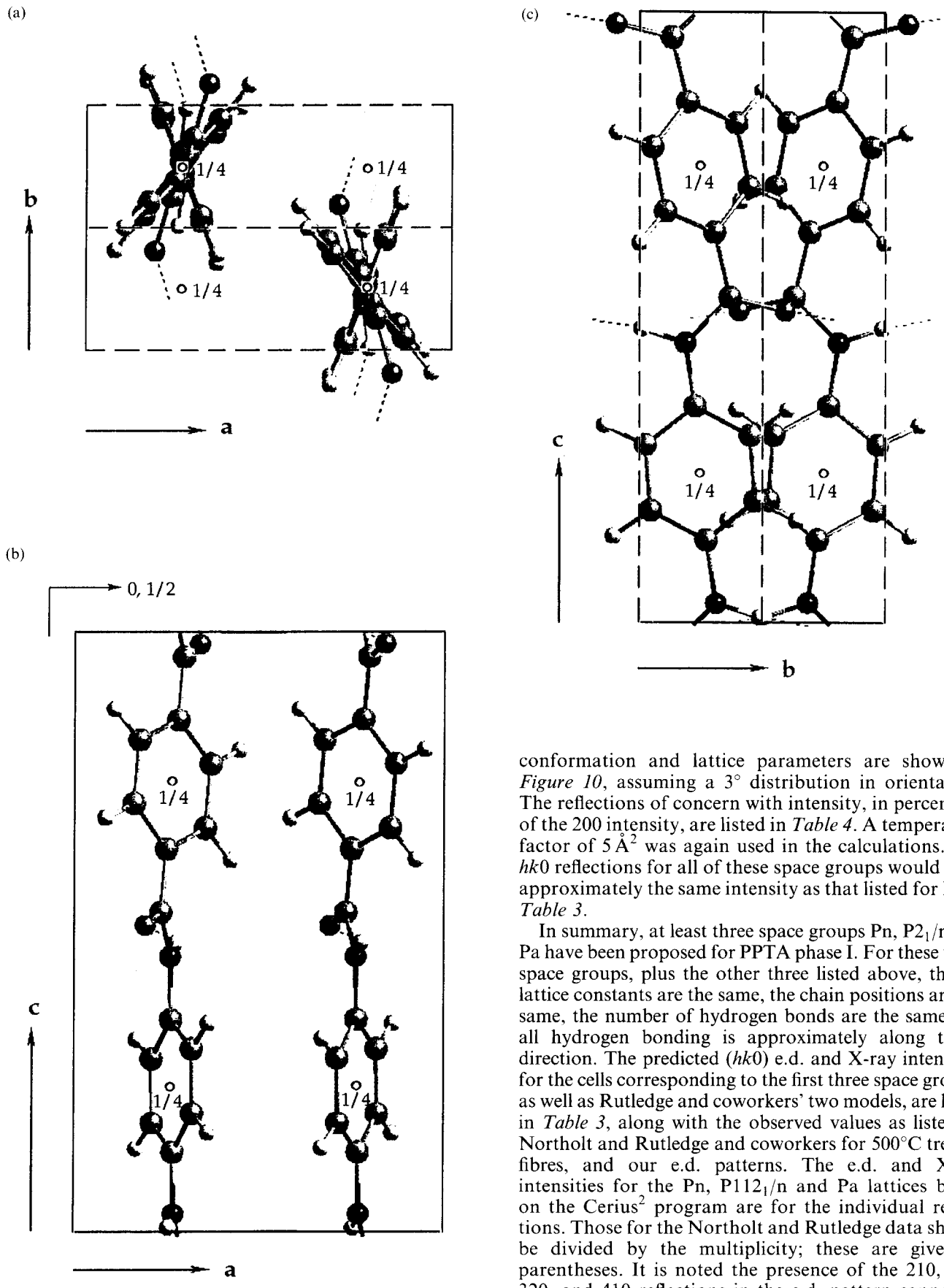

Figure 8 PPTA crystal structure (Pa) proposed in this work: (a) [001] projection; (b) [010] projection; (c) [100] projection

conformation and lattice parameters are shown in *Figure 10*, assuming a 3° distribution in orientation. The reflections of concern with intensity, in percentage of the 200 intensity, are listed in *Table 4*. A temperature factor of 5 $Å^2$ was again used in the calculations. The *hk*0 reflections for all of these space groups would have approximately the same intensity as that listed for Pa in *Table 3*.

In summary, at least three space groups Pn, $P2_1/n$ and Pa have been proposed for PPTA phase I. For these three space groups, plus the other three listed above, the six lattice constants are the same, the chain positions are the same, the number of hydrogen bonds are the same and all hydrogen bonding is approximately along the *b* direction. The predicted (*hk*0) e.d. and X-ray intensities for the cells corresponding to the first three space groups, as well as Rutledge and coworkers' two models, are listed in *Table 3*, along with the observed values as listed by Northolt and Rutledge and coworkers for 500°C treated fibres, and our e.d. patterns. The e.d. and X-ray intensities for the Pn, $P112_1/n$ and Pa lattices based on the Cerius[2] program are for the individual reflections. Those for the Northolt and Rutledge data should be divided by the multiplicity; these are given in parentheses. It is noted the presence of the 210, 120, 320, and 410 reflections in the e.d. pattern cannot be attributed to double diffraction. We suggest that the e.d. and X-ray data are in excellent agreement with the calculated values for our proposed cell.

Figure 11 is an e.d. pattern, frequently seen, from areas

(a)

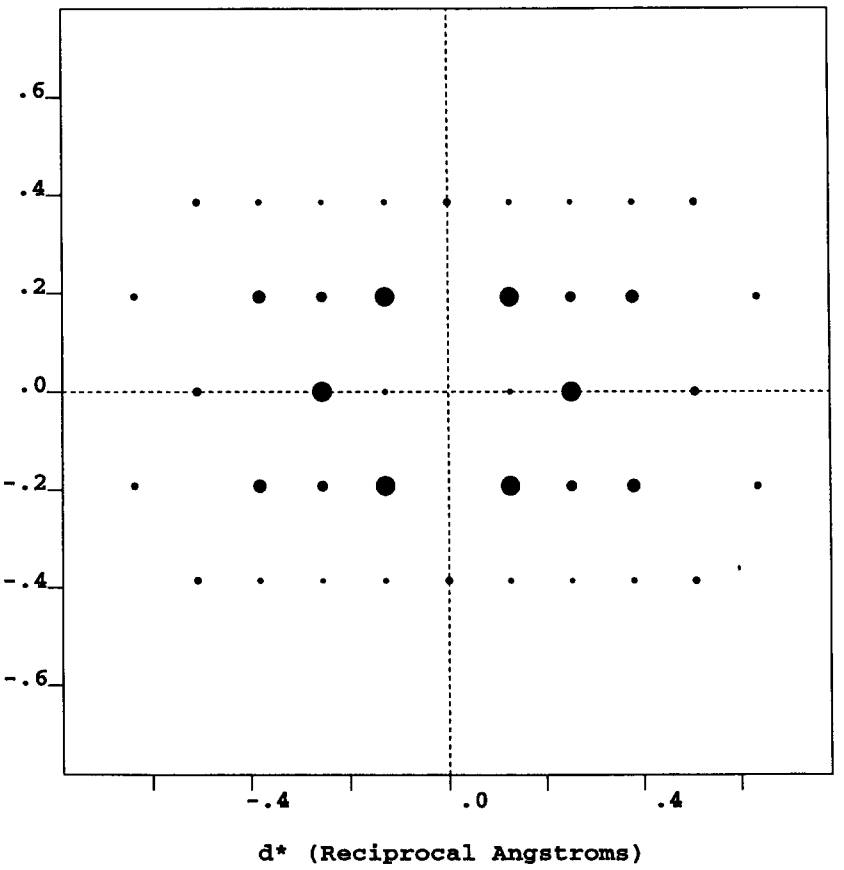

(b)

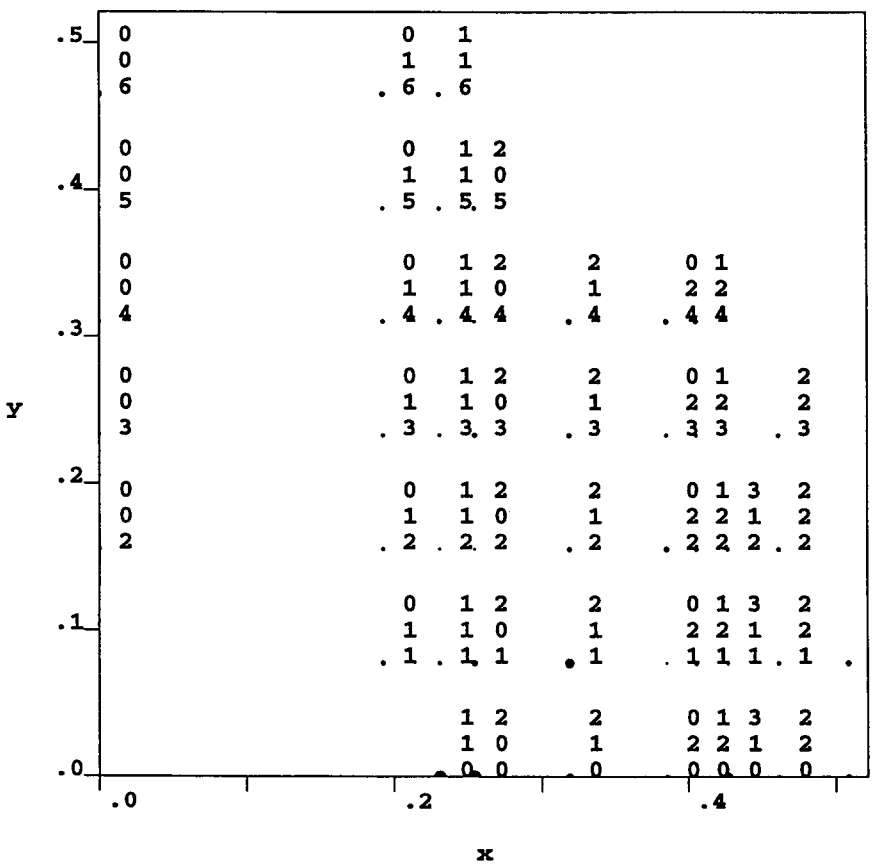

Figure 9 Simulated PPTA e.d. patterns based on the structure in *Figure 8*; (a) [001] zone; (b) fibre pattern. A simulated cylindrical X-ray fibre pattern is shown in (c). In the X-ray fibre pattern most 00*l* reflections are not seen since only a 3° distribution in orientation was assumed

(c)

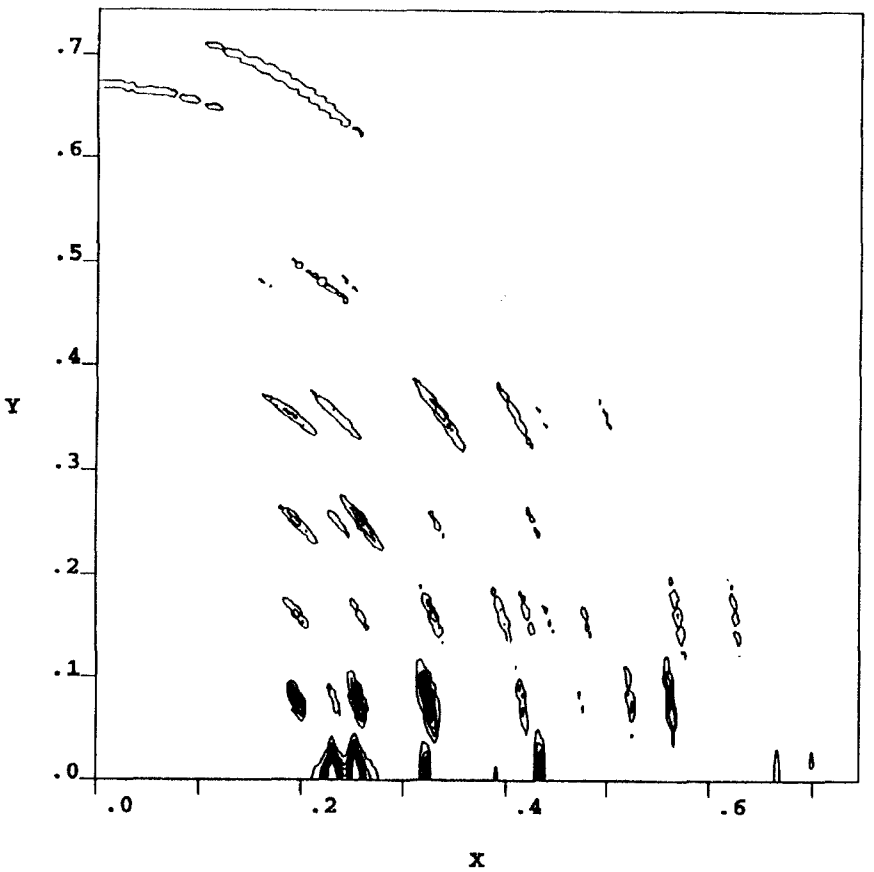

Figure 9 (*Continued*)

of poorly defined morphology. It appears to correspond to two single crystal patterns rotated by 93.5°. We have not, however, been able to define the corresponding unit cell. The spacings, in order of decreasing d, are 5.00, 4.36, 3.94 and 3.17 Å. The latter three agree well with the 110, 200 and 210 reflections (d = 4.33, 3.94 and 3.14 Å) based on our single crystal patterns, suggesting that the same unit cell is involved, which is possibly tilted. However, the only two reflections with d-values close to 5.00 Å are 102 (d = 4.99 Å) and 011 (d = 4.81 Å). It is noted the 5.00 Å reflections are in line with 200, suggesting it is 102, with a tilt about b, but the calculated maximum intensity with a 1/4 c shift between the hydrogen-bonded planes is only 1% of 200, whereas in the pattern it is stronger. While this could be due to the amount of tilt involved, one might expect the 110 reflections to also be substantially reduced in intensity and they do not appear to be; these patterns were taken under approximately the same exposure conditions as those in *Figure 5*. We note, in attempting to relate this pattern to phase II, that beginning with the molecules in the conformations and positions proposed by Hariguchi *et al.*[5], the Cerius[2] program moves them to the positions in phase I during energy minimization. Thus, at present our only suggestion for the origin of this pattern is that it is related to some type of tilting and 'twinning' of the planar crystals shown in *Figure 2*; the angle between the two upper, long growth faces is 94°, in agreement with the relation of the e.d. pattern, but further study is needed.

Table 4 E.d. fibre pattern intensities calculated for Pa, Pb, $P12_11$ and P1n1 space group models (expressed as percentages of the 200 intensity)

Reflections[a]	Pa	Pb	$P12_11$	Pn11
101	0	0.8	1.1	0.3
102	0	0.02	0.02	0.03
103	0	0.9	1.1	0.3
104	0	0.1	0.04	0.07
105	0	0.8	1.1	0.3
106	0	0.5	1.1	0.5
003	0.1	0.1	0	0
005	0.2	0.2	0.02	0
011	2.1	0	0.9	3.1
100	0	0	0.01	0
210	7.7	7.5	7.6	7.9
211	31.0	30.2	0.2	1.0

[a] These intensities are for reflections on fibre patterns. Thus 210 will have twice the value relative to 200 as on a single crystal pattern (as in *Table 3*) and intensities on the meridian and quadrants are reduced due to the curvature of the sphere of reflection

The fibre e.d. pattern is much more diffuse and has many fewer $hk0$ reflections than the single crystal e.d. pattern. This we find to typically be the case for samples sheared after polymerization. In the latter case, for chains with a direction (such as poly(*p*-oxybenzoate) or polybenzamide) it may be that the chain directions are statistical, whereas in the as-grown single crystals we have suggested a parallel alignment. That would not seem to apply in this case, with the chains being centrosymmetric. It is possible, however, that there is a statistical distribution of various types of chain packing. Furthermore, the agreement with the simulated e.d. fibre

(a)

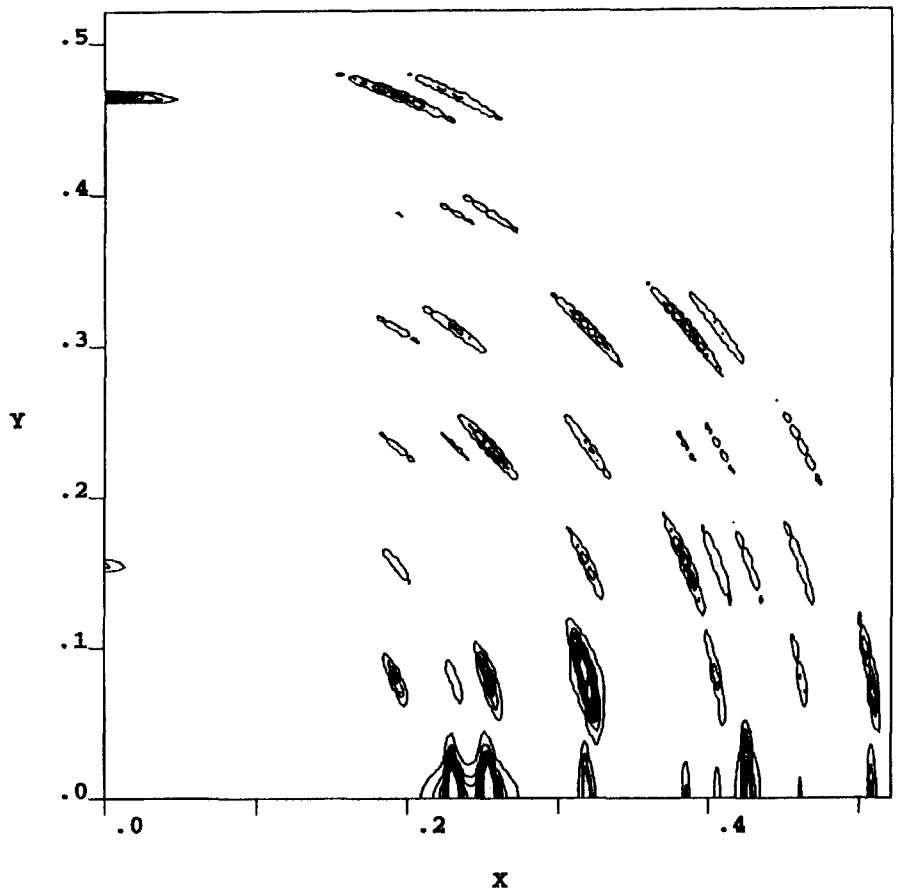

(b)

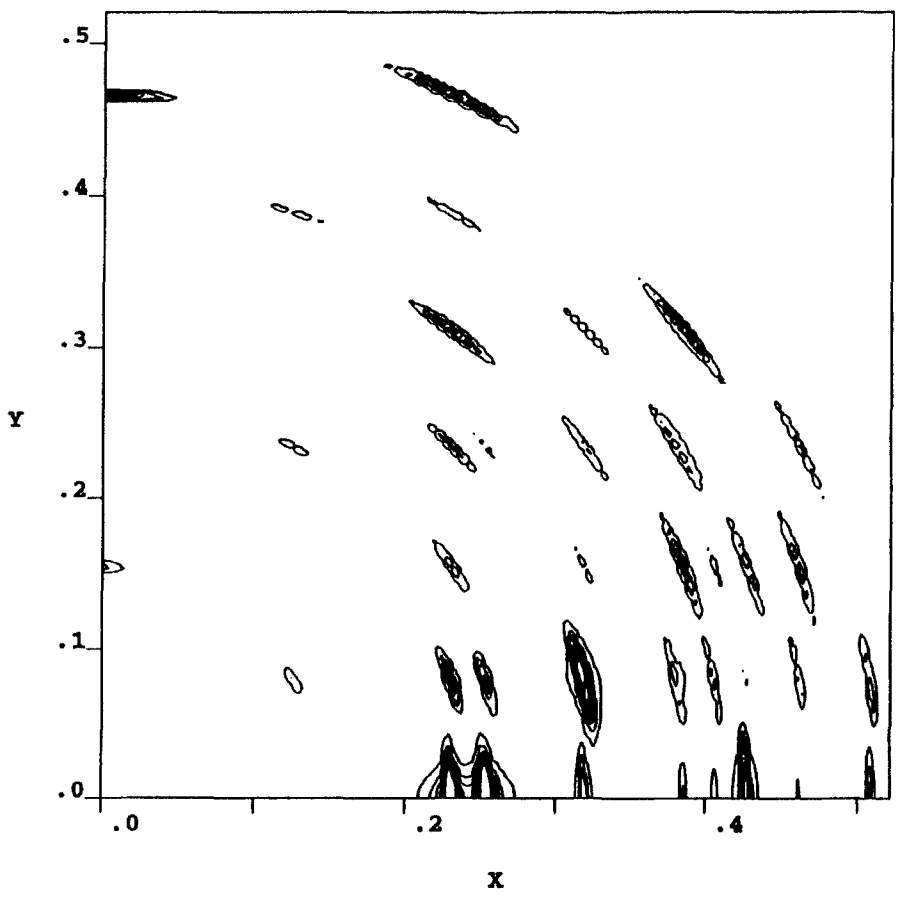

Figure 10 Simulated e.d. fibre patterns of the Pa, Pb, $p12_11$, and Pn11 space groups; a 3° distribution in orientations was assumed

(c)

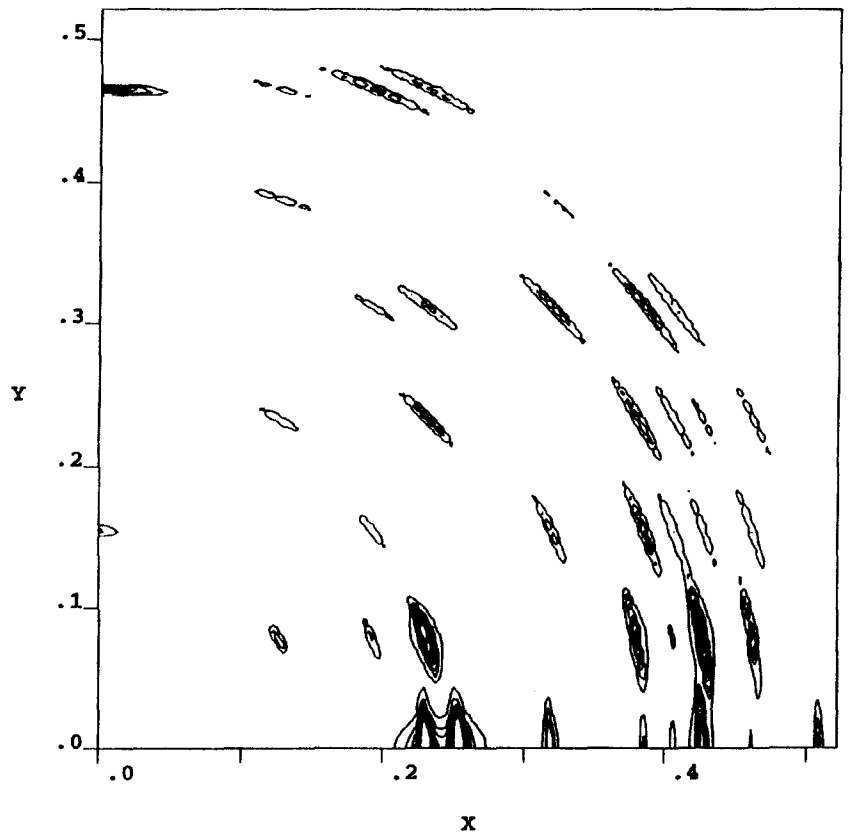

(d)

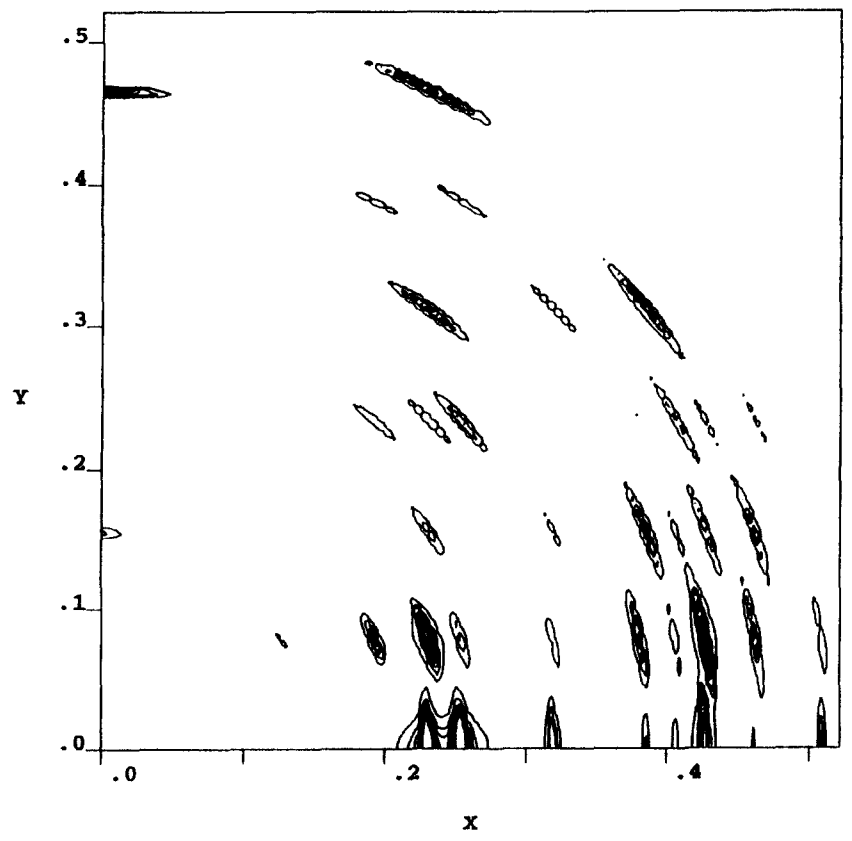

Figure 10 (*Continued*)

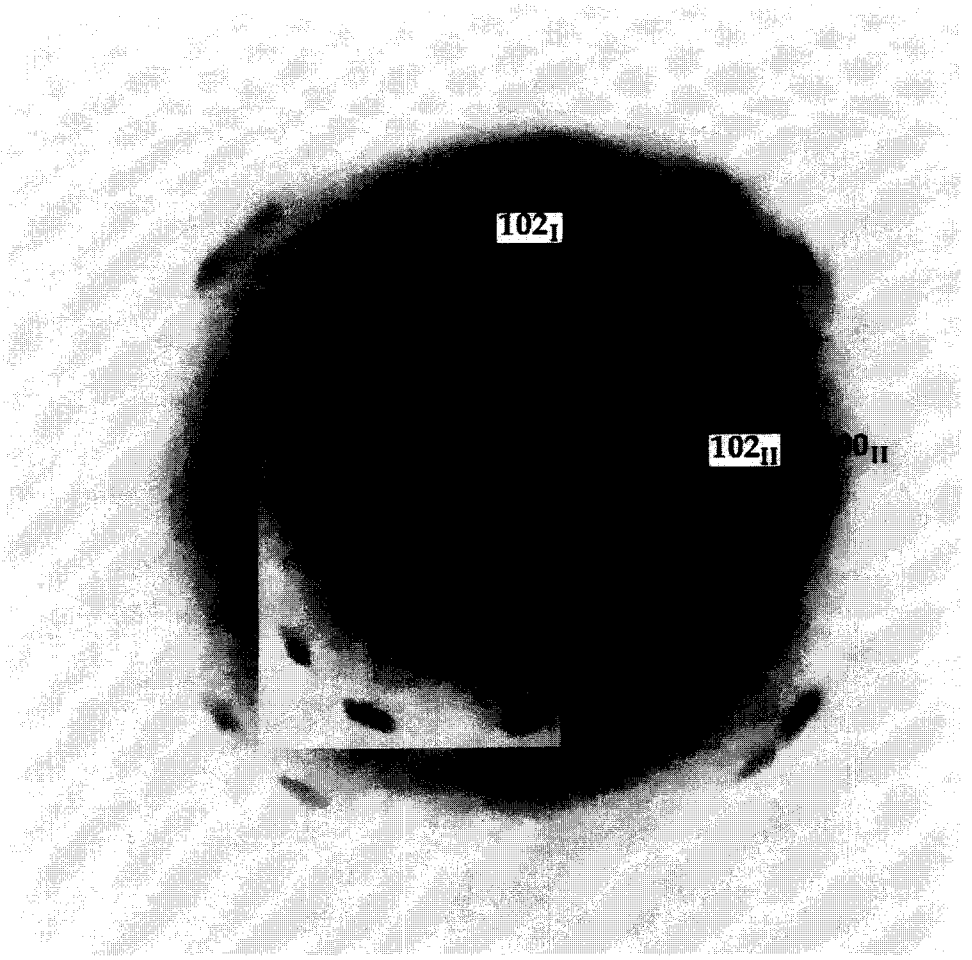

Figure 11 PPTA e.d. pattern frequently seen from material of poorly defined morphology

pattern, in particular the relative 002, 004, 006, 211, and 011 reflection intensities, suggest that the packing we propose is present even in the sheared (monomer) samples; in fact it is this we used to discriminate between the four possible space groups based on the *hk*0 pattern alone.

At this present time we have no explanation for the two types of morphologies observed. Both appear to have the same e.d. pattern.

CONCLUSIONS

The CTFMP technique has been shown to be useful for the growth of PPTA single crystals. Two types have been found. In the planar crystals we suggest the molecular length is equal to the crystal thickness, with monomer (or chemical repeat unit) addition on the surface as growth occurs. In the lath-shaped crystals a uniform thickness is observed over the entire area of the crystal; this is similar to the results we have observed for many other CTFMP grown crystals[23–32] and still remains to be explained.

The e.d. patterns are shown to agree most closely with a newly proposed unit cell have Pa symmetry. The predicted intensities are similar to those previously proposed for most reflections, but a number of them appear to be in better agreement with those we have observed rather than the corresponding predictions by Northolt[2] and Tadokoro and coworkers[3,4]. These include, in particular, the $h+k$ odd *hk*0 reflections which are absent for the previous two cells.

None of the cells proposed by Rutledge and co-workers[14,15] show reasonable agreement. It is also noted that our proposed cell would appear to be in agreement with Northolt's report of $h+k$ odd reflections in a 400°C annealed fibre. As suggested by Northolt, these results apply to our particular sample; it is highly likely that variations in packing may occur depending on sample preparation, e.g. crystal growth during polymerization vs. deformation of previously crystallized material vs. annealing of the latter.

ACKNOWLEDGEMENTS

This research was supported by funds from the Du Pont Co. (J. L.), a Presidential Young Investigators Award from the National Science Foundation (DMR-9175538) (S.Z.D.C.) at Akron, and a grant from the National Science Foundation (DMR-9312823) (J.L., P.H.G.) at Illinois.

REFERENCES

1 Trademark of E. I. du Pont de Nemours and Co. Inc.
2 Northolt, M. G. *Eur. Polym. J.* 1974, **10**, 799

3 Hasegawa, R. K., Chatani, Y. and Tadokoro, H. Proceedings of Meeting of the Crystallographic Society of Japan, Osaka, Japan, 1973, p. 21
4 Tashiro, K., Kobayashi, M. and Tadokoro, H. *Macromolecules* 1977, **10**, 413
5 Haraguchi, K., Kajiyama, T. and Takayanagi, M. *J. Appl. Polym. Sci.* 1979, **23**, 915
6 Dobb, M. G., Johnson, D. J. and Saville, B. P. *J. Polym. Sci. Polym. Symp. Edn* 1977, **58**, 237
7 Dobb, M. G., Johnson, D. J. and Saville, B. P. *J. Polym. Sci. Polym. Phys. Edn* 1977, **15**, 2201
8 Roche, E. J., Allen,S. R., Gabara, V. and Cox, B. *Polymer* 1989, **30**, 1776
9 Jackson, C. L. and Chanzy, H. D. *Polymer*, 1993, **34**, 5011
10 Takahashi, T., Yamamoto, T. and Tsujimoto, I. *J. Macromol. Sci. Phys.* 1979, **16**, 539
11 Hagege, R., Jarrin, M. and Sotton, M. *J. Microsc. (Part 1)* 1979, **115**, 65
12 Grubb, D. T., Prasab, K. and Adams, W. *Polymer* 1991, **32**, 1167
13 Snetivy, D., Vancso, G. J. and Rutledge, G. C. *Macromolecules* 1992, **25**, 7037
14 Rutledge, G. C. and Suter, U. W. *Macromolecules* 1992, **24**, 1921
15 Rutledge, G. C., Suter, U. W. and Papaspyrides, C. D. *Macromolecules* 1991, **24**, 1934
16 Woodward, A. D., Landis, J. and Frosini, V. *J. Polym. Sci. Polym. Phys. Edn* 1972, **10**, 2051
17 English, A. D. *J. Polym. Sci. Polym. Phys. Edn* 1986, **24**, 805
18 Schadt, R. J., Cain, E. J., Gardner, K. H., Garbara, V., Allen, S. R. and English, A. D. *Macromolecules* 1993, **26**, 6503
19 Schadt, R. J., Cain, E. J., Gardner, K. H., Garbara, V., Allen, S. R. and English, A. D. *Macromolecules* 1993, **26**, 6509
20 Shen, D. Y., Molis, S. E. and Hsu, S. L. *Polym. Eng. Sci.* 1983, **23**, 543
21 Chatzi, E. G., Urban, M. W., Ishida, H. and Koenig, J. L. *Polymer* 1986 **27**, 1850
22 Penn, L. and Milanovich, F. Polymer 1979, **20**, 31
23 Rybnikar, F., Liu, J. and Geil, P. H. *Macromol. Chem. Phys.* 1994, **195**, 81
24 Liu, J., Rybnikar, F. and Geil, P H. *J. Polym. Sci. Polym. Phys. Edn* 1992, **30**, 1469
25 Liu, J., Rybnikar, F., East, A. J. and Geil, P. H. *J. Polym. Sci. Polym. Phys. Edn* 1993, **31**, 1923
26 Rybnikar, F., Yuan, B.-L. and Geil, P. H. *Polymer* 1994, **35**, 1831
27 Rybnikar, F. and Geil, P. H. Paper presented at American Physical Society Meeting, Pittsburg, PA, March 1994
28 Liu, J., Chen, S. Z. D., Hsiao, B. and Gardner, K. *Macromolecules* 1994 **27**, 989
29 Liu, J., Kim, D., Harris, F. and Cheng, S. Z. D. *J. Polym. Sci. Polym. Phys. Edn* 1994, **32**, 2705
30 Liu, J., Kim, D., Harris, F. and Cheng, S. Z. D. *Polymer* 1994, **35**, 4048
31 Dean, D. and Geil, P. H. Paper presented at American Physical Society Meeting, Pittsburg, PA, March 1994, to be published
32 Long, J. C., Liu, J., Yuan, B.-L. and Geil, P. H. Paper presented at American Physical Society Meeting, San Jose, CA, March 1995 and Europhysics Conference on Macromolecular Physics, Prague, July, 1995
33 Trademark of Molecular Simulations, Inc.
34 Tadokoro and coworkers did not list calculated or observed intensities. The intensities listed here would differ from those that they would calculate since the chain conformation differs slightly from that in their diagrams; the plane of the terepthalate ring in their diagram appears to be tilted at a greater angle to the *c*-axis than the *p*-phenylene diamine ring
35 Lin, J., Geil, P. H., Huh, S. M. and Jin, J. I. *Acta Polymerica*, in press